

Seasonal aspects of the recent pause in surface warming

Kevin E. Trenberth^{*}, John T. Fasullo, Grant Branstator and Adam S. Phillips

Factors involved in the recent pause in the rise of global mean temperatures are examined seasonally. For 1999 to 2012, the hiatus in surface warming is mainly evident in the central and eastern Pacific. It is manifested as strong anomalous easterly trade winds, distinctive sea-level pressure patterns, and large rainfall anomalies in the Pacific, which resemble the Pacific Decadal Oscillation (PDO). These features are accompanied by upper tropospheric teleconnection wave patterns that extend throughout the Pacific, to polar regions, and into the Atlantic. The extratropical features are particularly strong during winter. By using an idealized heating to force a comprehensive atmospheric model, the large negative anomalous latent heating associated with the observed deficit in central tropical Pacific rainfall is shown to be mainly responsible for the global quasi-stationary waves in the upper troposphere. The wave patterns in turn created persistent regional climate anomalies, increasing the odds of cold winters in Europe. Hence, tropical Pacific forcing of the atmosphere such as that associated with a negative phase of the PDO produces many of the pronounced atmospheric circulation anomalies observed globally during the hiatus.

Although the 2000s are by far the warmest decade on record, the rate of increase of global mean temperature since 2000 has slowed, regardless of the data source¹ (see Fig. 1, and also Supplementary Fig. 1 for northern winter aspects). A linear fit to the global mean temperatures after 1970 is quite good, and the biggest outlier is actually 1998, which was affected by substantial heat coming out of the ocean in association with the 1997/1998 El Niño event^{2,3}. Hence, the post-1998 perspective (Fig. 1) is contrived because it depends on the choice of the starting year. Nevertheless, it is vital to understand related interannual and decadal variability reflected in Fig. 1 and its regionality. The strongest pause in the rise in global mean surface temperatures is in the northern winter (Supplementary Fig. 1), and the main places that warming has not occurred is in much of the central and eastern Pacific Ocean¹ and over northern continents, especially Eurasia⁴. Here we explore the teleconnections that are key to understanding the global structure of the various atmospheric anomalies associated with the warming hiatus, taking into account their seasonality to better determine the atmospheric forcings and responses, and understand the northern winter changes. This also provides an important perspective on the driving forces behind the patterns, and assists in discerning consequences from causes.

Several analyses of the factors involved in the apparent hiatus in the rise of global mean surface temperatures after about 2000 have been performed. Although small contributions have come from changes in the total solar irradiance as the Sun has gone into a quieter phase since about 2004 (ref. 5) and from aerosols in both the stratosphere (from small volcanic eruptions) and more regionally from pollution in the troposphere⁶, more than half of the cause of the hiatus is apparently associated with internal climate variability^{1,7–9} that we explore here.

Pacific decadal variability: seasonal signals

The phenomenon playing the main role is the PDO (refs 1,9), alternatively known from a slightly different perspective as the Interdecadal Pacific Oscillation, although it may not be a

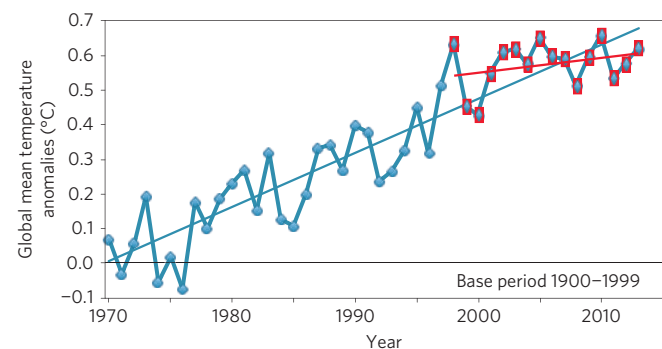


Figure 1 | Global mean surface temperature from NOAA, as anomalies relative to 1900–1999 plotted with linear trends for 1970–2013 (blue) and 1998–2013 (red).

quasi-linear mode of natural variability¹⁰. The PDO was in a negative phase before 1976, but became positive from 1976 to 1998, a period coinciding with strong increases in global mean surface temperatures^{1,11}. Then it switched to a negative phase in 1999 coinciding with the pause in upward trend in global mean surface temperatures. However, since 1999, the deeper ocean below 700 m has taken up more heat and there has not been a reduction in the Earth's energy imbalance^{3,8}.

The PDO pattern (Fig. 2) emerges from an analysis of the departures from the global mean of sea surface temperature (SST) monthly anomalies using a core region from 20° to 70° N, 110° E to 100° W for an empirical orthogonal function analysis^{1,11}. The base period is 1900–2012. The PDO/Interdecadal Pacific Oscillation has a Pacific-wide pattern in both surface and subsurface temperatures with an El Niño-like pattern throughout the tropics and strong extratropical links in both hemispheres (Fig. 2). The subsequent analysis only uses the PDO to provide markers for specifying the last two climate regimes: 1999–2012 versus 1976–1998 (ref. 1). This is more robust than using short-term linear trends⁹, although

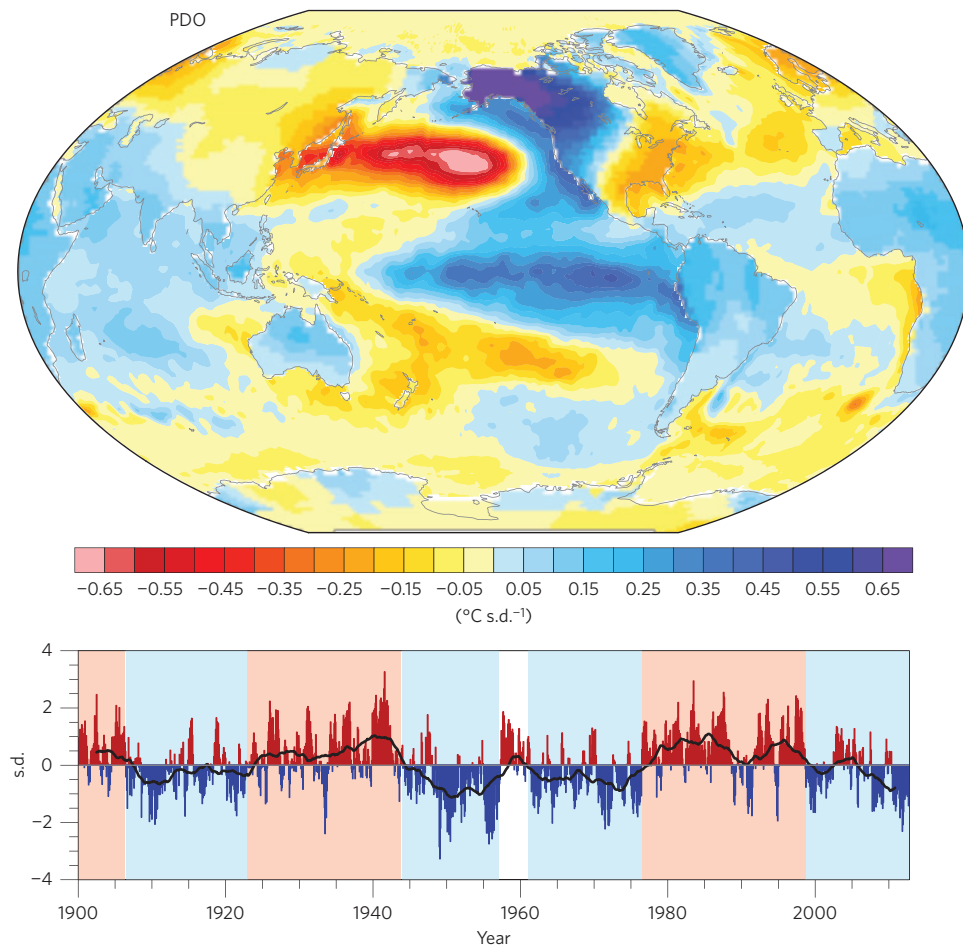


Figure 2 | The PDO based on an empirical orthogonal function analysis of SST anomalies with the global mean removed from 1900 to 2012 in the 20°–70° N, 110° E–100° W region of the North Pacific, which explains 25% of the variance. The principal component time series, given below in normalized units, is regressed on global sea and land surface temperature anomalies to give the map above. The black curve is a 61-month running average. The light red and blue colours depict the positive and negative phases of the PDO. Note the reversal of the colour key in the top panel so that blue colours are positive, and hence the current negative phase has below-normal SSTs in the blue areas. Here, s.d. is standard deviation.

results are similar. The recent PDO signals for the annual means¹ are complemented here with further diagnostic fields, including especially precipitation and atmospheric diabatic heating.

Since 1999 the annual mean tropical Pacific easterly trade winds have been much stronger than normal^{1,9} (see also Fig. 3). In the tropics and subtropics this coincides with striking sea-level pressure anomalies that relate to the Southern Oscillation. Much deeper warm waters have piled up in the western Pacific while cooler waters have prevailed through the top 500 m in the eastern Pacific¹. The result has been an increase in sea level of order 20 cm near the Philippines, but slight falls in the east since about 1999 (ref. 12), accompanied by changes in ocean heat content¹.

The pronounced strengthening in Pacific trade winds in the 2000s was unprecedented after 1979 and not captured by 48 climate model projections^{3,9} but was sufficient to account for the cooling of the tropical Pacific and a substantial slowdown in global surface warming through increased subsurface ocean heat uptake. While the strongest anomalies were indeed in the Pacific, strong connections also existed to the North Atlantic and southern oceans where subsurface ocean heat uptake penetrated to well below 700 m depth¹, altering surface winds and the distribution of Antarctic sea ice¹³, and the winter weather throughout Europe and North America. In the Pacific, the extra uptake came about through increased subduction in the Pacific shallow overturning cells, enhancing heat convergence in the equatorial thermocline^{9,14,15}.

Surface temperature (data sets are described in Supplementary Information) differences (Fig. 3a,b) clearly show that the central and eastern Pacific has failed to warm in the past 14 years, in a pattern associated with the PDO. To show the seasonality, two extended seasons November–March (NDJFM), northern winter, and May–September (MJJAS), northern summer, are examined. The Pacific cooling is stronger in northern winter (Fig. 3a). In general, surface warming deviates considerably from the PDO pattern outside the Pacific basin, perhaps signalling a substantial role for external forcing of the climate system and other factors such as internal variability beyond that associated with the PDO.

Precipitation differences between these two regimes (Fig. 3e,f) feature patterns similar to those associated with La Niña: much drier from 160° E to South America along the Equator, a northward-shifted but weaker northern Intertropical Convergence Zone, a southwestward-shifted South Pacific Convergence Zone, and extensive heavy rains over the Indonesian maritime continent. Wet conditions over northern Australia, Southeast Asia, northern Brazil, Colombia and Venezuela extend over the tropical Indian and Atlantic oceans (Supplementary Fig. 2) and are probably associated with changes in the Walker circulation¹⁶. The subtropical Pacific dry zone extends across the southeastern United States and throughout much of the North Atlantic in winter. Considering that the differences in Fig. 3 are for a 14-year period, the extent of the values exceeding 1 mm d⁻¹ is exceedingly large ($p < 0.05$ based on

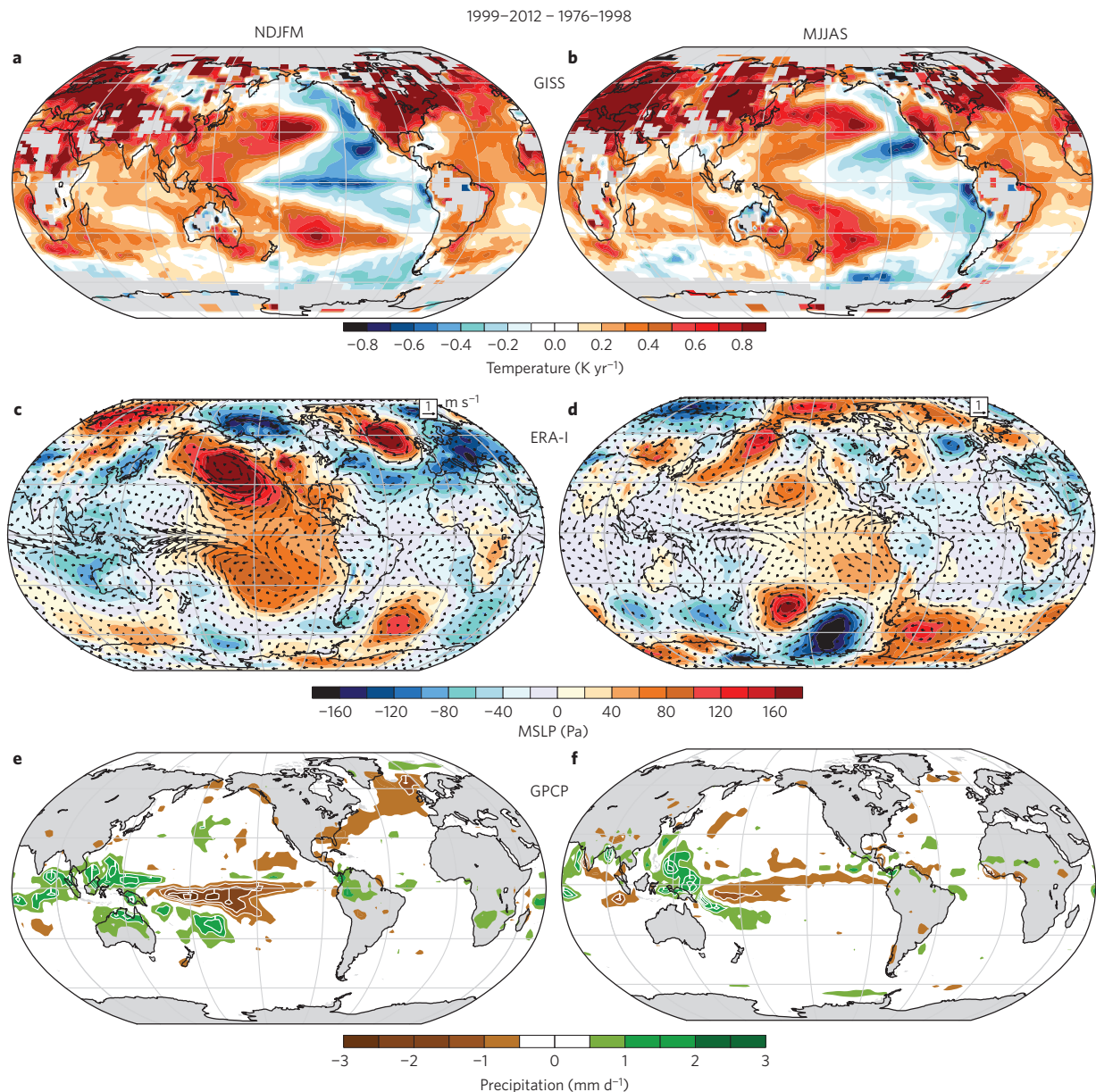


Figure 3 | Regime differences between 1999–2012 and 1976–1998. **a–f**, Mean differences between 1999–2012 and 1979–1998 for NDJFM (left) and MJJAS (right) for surface temperature from GISS (**a,b**), mean sea-level pressure (MSLP) differences from ERA-I (colours) and surface wind vectors (at 10 m, \mathbf{V}_{10} , arrows) with the key at the top right (**c,d**), and precipitation from GPCP truncated to T63 resolution (**e,f**). GISS: Goddard Institute for Space Studies; ERA-I: European Centre for Medium-range Weather Forecasts atmospheric reanalysis ERA-Interim; GPCP: Global Precipitation Climatology Project v2.2; see Supplementary Information.

the interannual standard deviation in the tropical Pacific from 1979 to 1995¹⁷ and two-sided Student's *t*-test), and suggests that much greater values occur in some years.

Complementary perspectives provided by the changes in sea-level pressure and surface winds (Fig. 3c,d) have some similarity in the tropical Pacific in both seasons, with a positive Southern Oscillation Index, but exhibit stronger anomalies in NDJFM. In the tropics, the intensification of easterly winds just south of the Equator near the Date Line in NDJFM exceeds 2 m s^{-1} versus about 1.1 m s^{-1} in MJJAS. These compare with mean vector wind speeds of up to 8 m s^{-1} in December–February and less than 7 m s^{-1} in June–August for 1950–1979¹⁸. Seasonal mean standard deviations are mostly less than 1 m s^{-1} , and hence an anomaly of 1 m s^{-1} over 14 years is highly statistically significant ($p < 0.01$). Sea-level pressure anomalies are large in both hemispheres in the subtropics, but stronger wave-like teleconnections in each hemisphere occur in winter.

The regime differences for the diabatic heating from radiation and latent and sensible heating of the atmosphere (Fig. 4) have been computed as a residual of the energy equations using ERA-I data^{19,20}. As 1 mm d^{-1} is equivalent to latent heating of about 29 W m^{-2} , its dominant role in the anomalous diabatic heating is apparent from comparing Fig. 3e,f with Fig. 4, and it is where precipitation anomalies exceed at least 0.5 mm d^{-1} over broad areas that a significant decadal response in terms of atmospheric teleconnections can be expected^{21,22}.

The degree to which the extratropical signal is wave-like in sea-level pressure is better seen in a polar projection (Supplementary Fig. 3). The alternating anomalies are clearest in MJJAS in the Southern Hemisphere. However, wave-like responses are best seen in the upper troposphere in the streamfunction field. Accordingly, we focus on the 300 hPa streamfunction differences (Fig. 5), which depict the rotational part of the flow (the flow is along the contours).

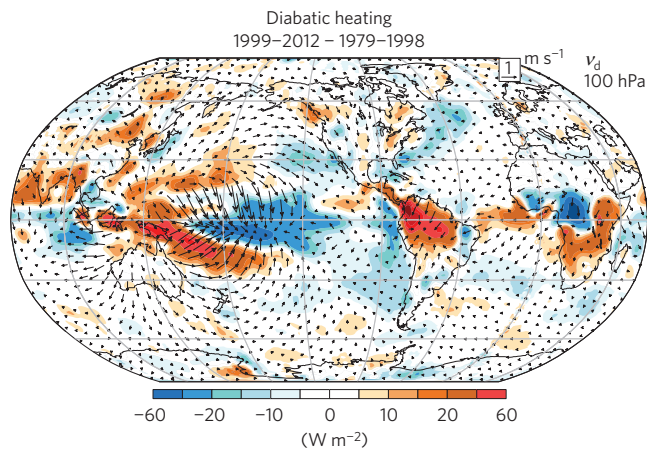


Figure 4 | Vertically integrated diabatic heating and divergent wind component for the difference between 1999–2012 and 1979–1998.

Diabatic heating (W m^{-2}) is computed as a residual from the energy equation and lightly smoothed with a 4-point smoother. The vectors show the divergent wind component at 100 hPa for the annual means, based on ERA-I reanalyses.

By far the strongest feature is the dipole structure in the central tropical Pacific straddling both the Equator and the region of the strongest precipitation deficit. There is a single predominant centre in the upper tropospheric tropics of each hemisphere with a cyclonic sign, as expected in conjunction with strong meridional convergence into the equatorial region and subsidence²¹ which can be inferred from the divergent wind components at 100 hPa (Fig. 4). That convergence is consistent with local atmospheric overturning driven by precipitation latent heat anomalies. The negative heating anomalies associated with the exceptionally dry tongue along the Equator evidently dominate the atmospheric forcing (Fig. 4). The pattern outside the tropics is strongly suggestive of a wave train of Rossby waves emanating from these regions that are strongest in winter²¹, as indicated schematically by the green arrows. This pattern constructively interferes with the observed long-term trend in tropospheric circulation²³ in some regions, and destructively in others.

From theory and modelling^{21,22}, tropical SST anomalies in the central and western Pacific are very effective in driving robust extratropical atmospheric responses. High SST anomalies lead to low surface pressure and low-level moisture convergence that feeds high precipitation, and vice versa for low SST anomalies. The latent heat (Fig. 3e,f) release in turn drives overturning circulations brought about in part by anomalous Walker circulations (Figs 4 and 5) throughout the tropics, and forces extratropical Rossby waves through the anomalous upper-level divergence flow (Fig. 4) perhaps involving the lower stratosphere²⁴ in the extratropics. The term $\beta v'_d$ in the atmospheric vorticity equation, where β is the meridional gradient of the Coriolis parameter and v'_d is the anomalous divergent northerly wind component (Supplementary Information), makes a large contribution to driving the changes in the rotational flow^{19,25} owing to the large values of v'_d (Fig. 4).

The stationary Rossby waves tend to follow a great circle route, and in turn alter the mid-latitude storm tracks, transient eddy heat and momentum transports, and interact with orography and the climatological mean flow. Negative SST anomalies and associated local precipitation deficits tend to have effects of opposite sign.

Idealized model simulations of response

A climate model driven with specified observed PDO-related SSTs in the tropical central and eastern Pacific but freely coupled elsewhere⁷ replicated many atmospheric features associated with

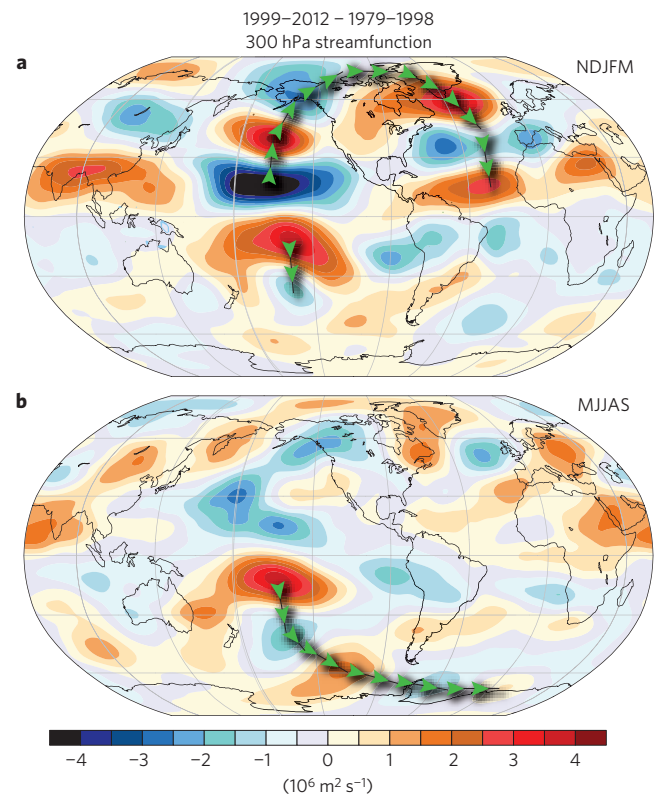


Figure 5 | The 300 hPa streamfunction for the differences between 1999–2012 and 1979–1998. a, NDJFM, and b, MJJAS, based on ERA-I reanalyses, where the rotational wind is parallel to the contours. The green arrowheads show schematically the main wave trains emanating from the tropical Pacific.

the PDO, including an enhanced Walker circulation and several seasonal aspects, although it also missed many important details of the summer precipitation anomalies (which was the only season presented). It did capture the drying over the US, although influences over the Atlantic, Arctic and Europe were not picked up.

To further provide evidence that the global response originates in the tropics, we have carried out several idealized experiments with the National Center for Atmospheric Research Community Atmospheric Model version 3 (CAM3; see Supplementary Information for details). Imposed heating (positive or negative) over a circle of half-amplitude radius of 750 km is placed on the Equator in runs that otherwise have climatological SSTs that vary only with day of year. The experiments have been run for 20 years, which is long enough for robust results, and compared with the mean climate of a 200-year control integration.

The model response varies with season. Results for cooling anomalies imposed on the Equator at 180° for NDJFM and at 165° W for MJJAS (Fig. 6), meant to mimic rainfall deficits, show the same seasonality seen in observations, with global upper-tropospheric wave trains being preferentially generated in the winter hemisphere of each season (Fig. 5). Moreover, many of the individual observed anomalies are also reproduced in the experiment, even as far away as the North and South Atlantic. The heating position does not make a substantial contribution to the seasonality of the response. As SSTs are imposed, some of the heat is dispersed into the ocean, whereas the rest is radiated to space at higher latitudes. Not only does this process force the planetary-scale waves, but the storm tracks are also altered and feedback onto the planetary waves through transient eddy heat and momentum fluxes to produce the final result. We have imposed a monopole of negative heating in the experiments whereas in the observations there is compensating heating at other

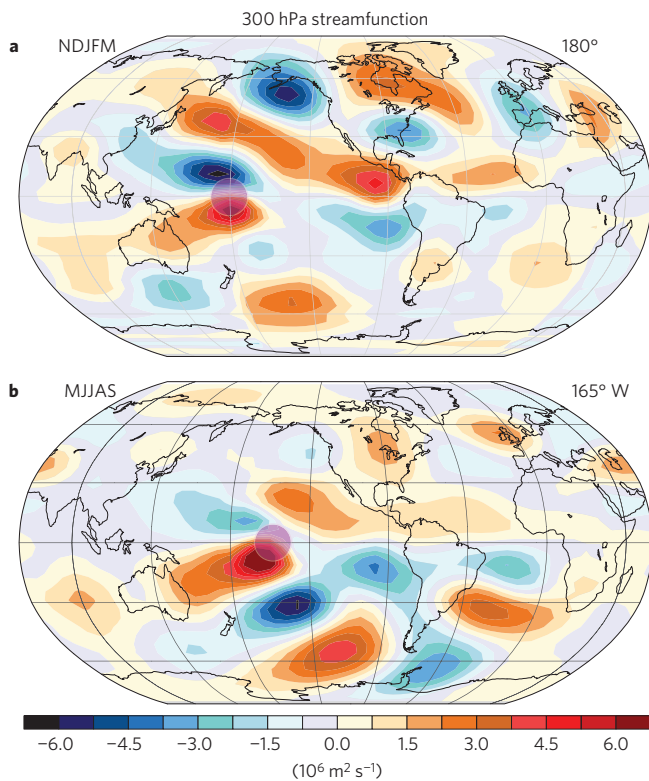


Figure 6 | Modelled 300 hPa streamfunction response. a,b, The streamfunction at 300 hPa response from CAM3 with circular heating on the Equator (pink circle showing the half-amplitude region) at 180° in NDJFM (**a**) and 165° W for MJJAS (**b**). The zonal mean has been removed.

longitudes. As a simple way to approximate its influence, we have removed the zonal mean (Fig. 6). The equivalent plot with the zonal mean included shows a more complex response, especially in the Northern Hemisphere for NDJFM (Supplementary Fig. 4).

Some studies have emphasized the western tropical Pacific as an effective region for forcing mid-latitudes^{26–28}, but we find for the hiatus that the central tropical Pacific is probably the dominant source region. A significant response to western Pacific heating would produce an upper tropospheric subtropical anticyclone but there is none in the hiatus pattern, consistent with the weak anomalous divergence in that region (Fig. 4). Moreover, CAM3 experiments (not shown) with idealized heating in the western Pacific do not produce a mid-latitude response that matches the mid-latitude hiatus pattern.

Although our experiments are idealized they include the key complex interactions within the atmosphere that occur in nature in the response, and serve to demonstrate certain properties of the climate system, but they are not intended to be a comprehensive simulation. Rather their merit lies in their simplicity and how well the results agree with observations. They strongly support the earlier interpretation that many of the atmospheric anomalies observed during the hiatus (Fig. 5) are probably forced from the tropics by the ocean.

The cause for the pause

Our results suggest that the hiatus in global mean temperature rise has been strongly influenced by the negative phase of the PDO. The planet is still warming⁸, but the changes in atmospheric circulation and surface winds, in particular, have changed ocean currents and more heat is being sequestered at greater depths. Effects are greatest in northern winter and there are profound regional manifestations. In particular, a cooler Europe is not reflected in

the regime shift patterns in Fig. 3a, and instead was related to a trend within the past epoch and cooler years after 2005 in winter^{1,4} (see Supplementary Fig. 1). In northern winter, teleconnections by means of quasi-stationary atmospheric Rossby waves forced from the tropical Pacific influenced the Arctic and predisposed the North Atlantic Oscillation to be in its negative phase (Figs 3c, 5a and 6a). In turn this favours cold outbreaks in Europe, as occurred in 2009–2010, 2010–2011 and 2012–2013 (Supplementary Fig. 5). These results help explain why the main absence of very recent warming over land has been over Eurasia in winter^{1,4}.

When atmospheric circulation patterns persist then there is generally anomalous atmospheric forcing, which mainly arises from anomalous SSTs that are most persistent in the central tropical Pacific. Indeed, our results demonstrate that tropical Pacific forcing of the atmosphere such as that associated with a negative phase of the PDO produces many of the pronounced atmospheric circulation anomalies observed globally during the hiatus. Tropical Pacific rainfall variations also occur on shorter timescales, including influences from the Madden–Julian Oscillation that are well established to influence the North Atlantic Oscillation^{29,30} and other transients, and from El Niño events on year-to-year timescales modulated by the PDO. Consequently, the exact teleconnections at any time vary substantially.

For instance in 2013–2014 northern winter, it has been speculated¹⁰ that increased greenhouse gases may have influenced the SSTs and helped trigger the substantial Rossby wave patterns of a strong ridge over the west coast of North America, a strong cold trough over the eastern United States and wet conditions over the United Kingdom. We note that the tropical Pacific rainfall during this winter featured very heavy rains near 160° E on the Equator associated with ‘westerly wind bursts’ and the developing El Niño event even though the dry region still existed in the central tropical Pacific.

Recent results³¹ suggest that these influences profoundly affected the Arctic, although that study was for annual means. We are able to replicate the essence of the teleconnections using a simple forcing in a full atmospheric model, whereas a coupled model⁷ did not realistically extend the patterns to the Arctic or North Atlantic. Much has been made of late about the atmosphere possibly becoming more ‘wavy’, and claims have been made that increased waviness is associated with loss of Arctic sea ice and Arctic amplification^{32,33}. Such claims have been disputed^{34–36}. Our results, and others^{28,31,37–39} suggest an alternative hypothesis where the warmer Arctic is a consequence, not a cause, of the wavy pattern through increased exchanges of cold air from the Arctic with warmer air from lower latitudes, in association with the teleconnections across the region that originated in the tropical Pacific. More fundamentally, the reason the Arctic is a less likely source of forced atmospheric waves is because heating influences from that region are much smaller in amplitude and less persistent. Precipitation and associated latent heat anomalies are an order of magnitude less than in the tropics.

In the Southern Hemisphere, the tropical Pacific SST has been found to affect the Antarctic from 1979 to 2009⁴⁰, although that study did not separate the effects into the two PDO regimes, as we have done here. The change in wave train after 1999 (Figs 3 and 5) is mainly in winter, and again is remarkably well simulated (Fig. 6) with an idealized forcing.

There is a strong predilection for anomalous atmospheric circulation conditions mainly in the winter of each hemisphere and in the subtropics of the summer hemisphere to arise from tropical Pacific SST anomalies. These have been recognized as a dominant mode of natural interannual variability associated with the El Niño/Southern Oscillation, but here we focused on the interdecadal variability that has become strongly evident recently through its manifestation as a pause in the rise of global mean temperatures. Accompanying the recent negative phase of the PDO

has been striking changes in tropical and subtropical winds and ocean currents, with profound effects on ocean heat content and sea level. Some of these aspects seem to be unique to the past decade and raise questions about whether natural internal variability itself is being altered by climate change.

Methods

Full Methods and associated references are available in the Supplementary Information.

Received 20 May 2014; accepted 11 July 2014;
published online 17 August 2014

References

- Trenberth, K. E. & Fasullo, J. T. An apparent hiatus in global warming? *Earth's Future* **1**, 19–32 (2013).
- Trenberth, K. E., Caron, J. M., Stepaniak, D. P. & Worley, S. The evolution of ENSO and global atmospheric surface temperatures. *J. Geophys. Res.* **107**, 4065 (2002).
- Balmaseda, M. A., Trenberth, K. E. & Källén, E. Distinctive climate signals in reanalysis of global ocean heat content. *Geophys. Res. Lett.* **40**, 1754–1759 (2013).
- Cohen, J. L., Furtado, J. C., Barlow, M., Alexeev, V. A. & Cherry, J. E. Asymmetric seasonal temperature trends. *Geophys. Res. Lett.* **39**, L04705 (2012).
- Schmidt, G. A., Shindell, D. T. & Tsigaridis, K. Reconciling warming trends. *Nature Geosci.* **7**, 158–160 (2014).
- Santer, B. *et al.* Volcanic contribution to decadal changes in tropospheric temperature. *Nature Geosci.* **7**, 185–189 (2014).
- Kosaka, Y. & Xie, S.-P. Recent global-warming hiatus tied to equatorial Pacific surface cooling. *Nature* **501**, 403–407 (2013).
- Trenberth, K. E., Fasullo, J. T. & Balmaseda, M. A. Earth's energy imbalance. *J. Clim.* **27**, 3129–3144 (2014).
- England, M. *et al.* Recent intensification of wind-driven circulation in the Pacific and the ongoing warming hiatus. *Nature Clim. Change* **4**, 222–227 (2014).
- Palmer, T. Record-breaking winters and global climate change. *Science* **344**, 803–804 (2014).
- Deser, C., Alexander, M. A., Xie, S.-P. & Phillips, A. S. Sea surface temperature variability: Patterns and mechanisms. *Ann. Rev. Mar. Sci.* **2**, 115–143 (2010).
- Merrifield, M. A., Thompson, P. R. & Lander, M. Multidecadal sea level anomalies and trends in the western tropical Pacific. *Geophys. Res. Lett.* **39**, L13602 (2012).
- Holland, P. R. & Kwok, R. Wind-driven trends in Antarctic sea-ice drift. *Nature Geosci.* **5**, 872–875 (2012).
- Meehl, G. A., Arblaster, J. M., Fasullo, J. T., Hu, A. & Trenberth, K. E. Model-based evidence of deep-ocean heat uptake during surface-temperature hiatus periods. *Nature Clim. Change* **1**, 360–364 (2011).
- Meehl, G. A., Hu, A., Arblaster, J. M., Fasullo, J. T. & Trenberth, K. E. Externally forced and internally generated decadal climate variability in the Pacific. *J. Clim.* **26**, 7298–7310 (2013).
- L'Heureux, M., Lee, S. & Lyon, B. Recent multi-decadal strengthening of the Walker Circulation across the tropical Pacific. *Nature Clim. Change* **3**, 571–576 (2013).
- Trenberth, K. E. & Guillemot, C. J. Evaluation of the atmospheric moisture and hydrological cycle in the NCEP/NCAR reanalyses. *Clim. Dynam.* **14**, 213–231 (1998).
- Halpert, M. S. & Ropelewski, C. F. Atlas of tropical sea surface temperature and surface winds. *NOAA Atlas No. 8* (1989).
- Trenberth, K. E. & Stepaniak, D. P. Co-variability of components of poleward atmospheric energy transports on seasonal and interannual timescales. *J. Clim.* **16**, 3691–3705 (2003).
- Trenberth, K. E. & Stepaniak, D. P. Seamless poleward atmospheric energy transports and implications for the Hadley circulation. *J. Clim.* **16**, 3706–3722 (2003).
- Trenberth, K. E. *et al.* Progress during TOGA in understanding and modeling global teleconnections associated with tropical sea surface temperatures. *J. Geophys. Res.* **103**, 14291–14324 (1998).
- Barsugli, J. J. & Sardeshmukh, P. D. Global atmospheric sensitivity to tropical SST anomalies throughout the Indo-Pacific basin. *J. Clim.* **15**, 3427–3442 (2002).
- Teng, H. & Branstator, G. A zonal wavenumber 3 pattern of Northern Hemisphere wintertime planetary wave variability at high latitudes. *J. Clim.* **25**, 6756–6769 (2012).
- Butler, A. H., Polvani, L. M. & Deser, C. Separating the stratospheric and tropospheric pathways of El Niño–Southern Oscillation teleconnections. *Environ. Res. Lett.* **9**, 024014 (2014).
- Seo, K.-H. & Son, S.-W. The global atmospheric circulation response to tropical diabatic heating associated with the Madden–Julian Oscillation during northern winter. *J. Atmos. Sci.* **69**, 79–96 (2012).
- Simmons, A. J., Wallace, J. M. & Branstator, G. W. Barotropic wave propagation and instability and atmospheric teleconnection patterns. *J. Atmos. Sci.* **40**, 1363–1392 (1983).
- Palmer, T. N. & Mansfield, D. A. Response of two atmospheric general circulation models to sea-surface temperature anomalies in the tropical East and West Pacific. *Nature* **310**, 483–485 (1984).
- Lee, S., Gong, T. T., Johnson, N. C., Feldstein, S. B. & Pollard, D. On the possible link between tropical convection and the Northern Hemisphere Arctic surface air temperature change between 1958–2001. *J. Clim.* **24**, 4350–4367 (2011).
- Cassou, C. Intraseasonal interaction between the Madden–Julian Oscillation and North Atlantic Oscillation. *Nature* **455**, 523–527 (2008).
- Lin, H., Brunet, G. & Derome, J. An observed connection between the North Atlantic Oscillation and the Madden–Julian Oscillation. *J. Clim.* **22**, 364–380 (2009).
- Ding, Q. *et al.* Tropical forcing of the recent rapid Arctic warming in northeastern Canada and Greenland. *Nature* **509**, 209–213 (2014).
- Francis, J. A. & Vavrus, S. J. Evidence linking Arctic amplification to extreme weather in mid-latitudes. *Geophys. Res. Lett.* **39**, L06801 (2012).
- Tang, Q., Zhang, X. & Francis, J. A. Extreme summer weather in northern mid-latitudes linked to a vanishing cryosphere. *Nature Clim. Change* **4**, 45–50 (2014).
- Barnes, E. A. Revisiting the evidence linking Arctic amplification to extreme weather in midlatitudes. *Geophys. Res. Lett.* **40**, 4734–4739 (2013).
- Barnes, E. A., Dunn-Sigouin, E., Masato, G. & Woollings, T. Exploring recent trends in Northern Hemisphere blocking. *Geophys. Res. Lett.* **41**, 638–644 (2014).
- Wallace, J. M., Held, I. M., Thompson, D. W. J., Trenberth, K. E. & Walsh, J. E. Global warming and winter weather. *Science* **343**, 729–730 (2014).
- Yoo, C., Feldstein, S. & Lee, S. Impact of the Madden–Julian Oscillation (MJO) trend on the polar amplification of surface air temperature during 1979–2008 boreal winter. *Geophys. Res. Lett.* **38**, L24804 (2011).
- Lee, S. Testing of the tropically excited Arctic warming (TEAM) mechanism with traditional El Niño and La Niña. *J. Clim.* **25**, 4015–4022 (2012).
- Lee, S. A theory for polar amplification from a general circulation perspective. *Asia-Pacific J. Atmos. Sci.* **50**, 31–43 (2014).
- Ding, Q., Battisti, D. S. & Küttel, M. Winter warming in West Antarctica caused by central tropical Pacific warming. *Nature Geosci.* **4**, 398–403 (2011).

Acknowledgements

The National Center for Atmospheric Research is sponsored by the National Science Foundation. This research is partially sponsored by NASA under grant NNX09AH89G.

Author contributions

K.E.T. led the writing of the paper and conceived the study. J.T.F. and A.S.P. analysed the data to produce most of the figures, G.B. carried out the modelling. All authors contributed to data interpretation and writing of the manuscript.

Additional information

Supplementary information is available in the online version of the paper. Reprints and permissions information is available online at www.nature.com/reprints. Correspondence and requests for materials should be addressed to K.E.T.

Competing financial interests

The authors declare no competing financial interests.